

Conf-951033-4

SAND095-1496C

## DISCLAIMER

This report was prepared as an account of work sponsored by an agency of the United States Government. Neither the United States Government nor any agency thereof, nor any of their employees, makes any warranty, express or implied, or assumes any legal liability or responsibility for the accuracy, completeness, or usefulness of any information, apparatus, product, or process disclosed, or represents that its use would not infringe privately owned rights. Reference herein to any specific commercial product, process, or service by trade name, trademark, manufacturer, or otherwise does not necessarily constitute or imply its endorsement, recommendation, or favoring by the United States Government or any agency thereof. The views and opinions of authors expressed herein do not necessarily state or reflect those of the United States Government or any agency thereof.

RECEIVED

JUL 18 1995

OSTI

## SPUTTER DEPOSITION OF ZnS:Mn/SrS:Ce MULTILAYER STACKS FOR USE AS WHITE PHOSPHOR THIN FILM ELECTROLUMINESCENT PANELS

Judith A. Ruffner,

Sandia National Laboratories, Albuquerque, New Mexico 87185

Richard T. Tuenge and Sey-Shing Sun

Planar America, Inc., Beaverton, Oregon 97006

## ABSTRACT

Sputter deposition of ZnS:Mn/SrS:Ce multilayered broad-band "white" emission thin film electroluminescent (TFEL) stacks has been investigated. To date, deposition of these multilayers has been limited to vacuum evaporation techniques and atomic layer epitaxy, both of which require two different substrate temperatures for growth of high quality ZnS and SrS. This repeated thermal cycling during multilayer deposition can induce stress, defects, and interdiffusion which adversely affect EL performance.

Sputter deposition of ZnS and SrS produces high quality TFELs for a wider range of substrate temperatures. Both materials can be sputter deposited at a common temperature (300-350°C) which eliminates the need for thermal cycling and increases manufacturability. Luminance outputs from sputter deposited ZnS and SrS thin films are comparable to those from evaporated films, making sputtering an attractive alternative deposition technique for these materials.

We report on the effects of sputter deposition parameters including chamber pressure, substrate temperature, and H<sub>2</sub>S process gas partial pressure on the resultant composition and morphology of ZnS:Mn and SrS:Ce thin films and multilayers. Their EL performance was evaluated and correlated to composition and morphology.

KEY WORDS: Thin Films, Phosphors, Electroluminescent Displays

This work was supported by the United States Department of Energy under Contract #DE-AC04-94-AL-85000.

MASTER

DISTRIBUTION OF THIS DOCUMENT IS UNLIMITED

DLC

## **DISCLAIMER**

**Portions of this document may be illegible  
in electronic image products. Images are  
produced from the best available original  
document.**

## 1. INTRODUCTION

**1.1 TFEL Displays** Although TFEL displays represent only 2% of the annual sales in flat panel displays, they offer some important advantages over liquid crystal displays (LCDs) which are the present leader in world-wide sales (83%) (1). These advantages include excellent viewing properties, fast response time, and nearly constant luminance output over a wide temperature range (0 - 40°C).

TFEL displays are lambertian emitters which permit viewing from oblique angles of up to nearly 90° in all quadrants. They offer response times on the order of microseconds enabling rapid scrolling and cursor motion with no flicker or ghosting. These attributes make TFEL displays some of the most aesthetically appealing of all the flat panel display types. In addition, their temperature stability, low power consumption, minimum display depth, and intrinsic ruggedness which results from their solid state nature make small to medium sized (1 - 8" in diagonal) TFEL displays ideal for a wide variety of mobile applications. These applications include mobile military systems, head mounted displays, portable medical equipment, test and measurement equipment, telecom displays, and transportation system displays.

The "simple model" of the ac TFEL structure consists of a thin film phosphor (e.g. ZnS:Mn) sandwiched between transparent layers of an insulator (e.g., silicon oxynitride or aluminum titanium oxide) and a conductor (indium tin oxide) as shown in Figure 1a (2). When a voltage applied across the conductors exceeds a threshold value, electrons trapped at the dielectric/ phosphor (cathode) interface undergo tunnel emission out of the shallow traps. Because the field is very high, electrons do not lose kinetic energy to phonons and are ballistically accelerated across the phosphor layer (2). The electrons undergo two important processes in the phosphor layer: they can impact excite a luminescent center ( $Mn^{2+}$ ) which then de-excites radiatively to emit a photon of a characteristic wavelength, or they can impact-ionize a valence band electron to the conduction band in the host material to produce an electron-hole pair. The release of these additional electrons serves to increase the probability for impact excitation of the luminescent centers and plays an important role in luminescent output.

A multilayered structure that consists of two different phosphor materials, as shown in Figure 1b, can emit light of several different wavelengths to produce "white" light emission. In the structure shown, excitation of the SrS:Ce produces blue light centered at  $\lambda=480$  nm, while excitation of the ZnS:Mn produces a very intense emission centered at  $\lambda = 580$  nm. The emission spectrum of ZnS:Mn is so broad and so intense that it is possible to use color filters to "pick off" red and green components for use in a broad band display (3). As a result, these two phosphor materials can be interlayered to produce the red, green, and blue components for white light emission.

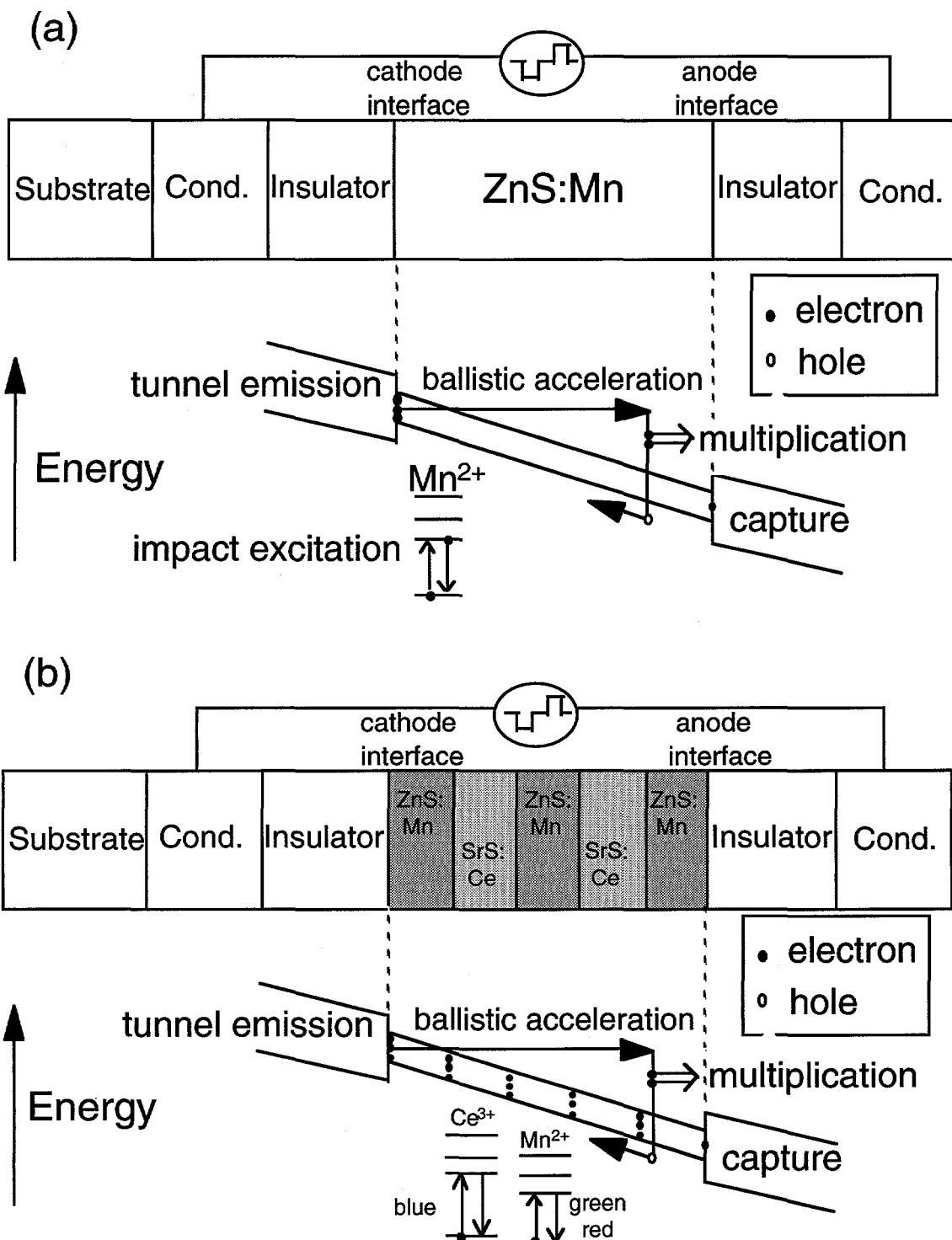


Figure 1 (a) The "simple model" and corresponding energy diagram of a TFEL device. (b) A multilayered "white" phosphor TFEL device. (2)

In addition to producing white light, the theory that electrons originate from the shallow interface traps suggests that a multilayered structure will produce higher luminance as a result of the additional electrons available from the shallow phosphor/phosphor interface traps. Mauch *et al.* studied several layered ZnS:Mn/SrS:Ce structures and found that luminance did increase with the number of multilayers for the same overall sample thickness as predicted (4-5).

An efficient white phosphor in a TFEL device offers the potential for the production of low cost, full-color flat panel displays with high definition. Compared to a three phosphor (RGB) patterned display panel, fabrication of a full color TFEL display that uses color filters in conjunction with a white phosphor would require significantly fewer vacuum thin film depositions and photolithographic patterning and etch steps. Color filter technology already developed for active matrix LCDs is expected to be transferable and cost effective for use in white phosphor TFEL displays.

**1.2 Sputter Deposition of Phosphor Films** Fabrication of a ZnS:Mn/SrS:Ce white phosphor multilayered structure requires a compatible deposition process for the two phosphor materials. Sputter deposition of the ZnS:Mn/SrS:Ce multilayered stack may be the most suitable technique because it enables deposition of both phosphor materials at a common temperature (300-350°C) as discussed in the following sections. This is in contrast to other vacuum evaporation techniques that require deposition of ZnS:Mn T < 275 °C and deposition of SrS:Ce at T > 600 °C. This thermal cycling during deposition is very inconvenient for production and increases the probability of mechanical failure due to the differential thermal expansion coefficients between the substrate, electrode, insulator, and phosphor layers. Sputtering offers several other advantages such as larger panel sizes, higher uniformity, higher film density, higher deposition rates, lower cost, and in-line manufacturing capabilities.

**1.2.1 ZnS:Mn** Thin films of ZnS:Mn for TFEL applications have been deposited using molecular beam epitaxy (6), atomic layer epitaxy (7), metal organic chemical vapor deposition (8), thermal evaporation (9), and rf sputtering (10-14). In the first four processes, the deposition rate of ZnS:Mn falls off dramatically for substrate temperatures > 275 °C because the sticking coefficients of evaporated species, mainly Zn and S<sub>2</sub> (9), approach zero. In contrast, sputtered species consist of Zn, S, MnS, ZnS, MnZn, Zn<sub>2</sub>, and Zn<sub>2</sub>S which maintain reasonably high sticking coefficients at much higher deposition temperatures (> 400 °C). As a result, ZnS:Mn can be sputter deposited at much higher substrate temperatures (13).

Thin films of ZnS:Mn were rf sputter deposited onto substrates held at temperatures ranging from 250 - 450 °C by Frey *et al.* (15). The resultant TFEL devices exhibited luminance values of > 27 fL and efficiencies of up to 2 lm/W at 60 Hz. The threshold voltage of these devices ranged from 300 - 350 V. Although these films offered high EL performance, they suffered from thickness and compositional variations across the display area which resulted in an average brightness nonuniformity of 25% over their displays. These variations were probably a result

of nonuniform heating of the substrate during deposition (15). Therefore, rf sputter deposited ZnS:Mn phosphor films offer high performance in TFEL displays but must be deposited in a manner that maximizes thickness and compositional uniformity.

**1.2.2 SrS:Ce** films have been deposited using reactive evaporation from Knudsen cells (4, 5, 16), e-beam evaporation (17), and rf sputtering (18-20). There are striking differences between the performance of SrS:Ce TFEL samples deposited by these various methods reported in the literature. However, the differences in EL performance are likely a result of significant differences in other thin film properties (such as microstructure and composition) that are a direct result of the deposition process itself (21). Sputtering appears to be a very promising technique for deposition of SrS:Ce phosphor films because it generally results in stoichiometric films at low substrate temperatures, and results in very high efficiencies (up to 1.3 lm/W) in TFEL devices. Further optimization of the doping concentration and rf sputter deposition conditions may result in much higher efficiencies of these TFEL displays (22).

Another advantage of sputtering is that it enables deposition of high crystalline quality, high EL performance SrS:Ce phosphor films at significantly lower substrate temperatures ( $T < 300$  °C) (20) than those required for evaporation deposition ( $T > 600$  °C) (23). The reduction in the required energy is most likely a result of the higher kinetic energies imparted to the adatoms during the sputtering process and is a critical factor in realizing a common deposition temperature for ZnS:Mn and SrS:Ce in a multilayered structure.

**1.2.3 ZnS:Mn/SrS:Ce Multilayered Phosphor Films** Multilayered depositions of ZnS:Mn/SrS:Ce have been reported by several research groups (4, 5, 24-26). Mauch *et al.* used reactive evaporation to fabricate 9-layer stacks of alternating ZnS:Mn and SrS:Ce phosphor layers. Although they reported high luminance values for the multilayered structure, their deposition technique required substrate temperatures of 200 °C and 600 - 650 °C for the ZnS:Mn and SrS:Ce layers respectively (4, 5). It is possible to avoid this thermal cycling for multilayered white phosphors by using sputter deposition at a common growth temperature.

## 2. EXPERIMENT

**2.1 Sputter Deposition of Phosphor Films** Thin films of ZnS:Mn and SrS:Ce phosphors are deposited using rf sputtering under a variety of deposition conditions. All thin film samples are deposited in a turbo-pumped Unifilm PVD-300 multisource sputtering system which has a base pressure of  $1 \times 10^{-7}$  torr. The chamber is fitted with a load-lock that enables rapid sample loading without exposing the inner chamber and water-sensitive SrS:CeF<sub>3</sub> target to atmospheric contamination. The pumping and exhaust mechanisms of the turbo pump enable the safe removal of hazardous process gases such as H<sub>2</sub>S from the chamber.

An extensive computer model and deposition control program is used to rotate and scan the sample with respect to the sputter target during deposition in order to maximize the thickness and compositional uniformity across the area of the substrate. This scanning algorithm enables us to routinely achieve 99% thickness uniformity across a sample up to 8" in diameter from a 3" diameter sputter target. The ability to achieve precise thickness and compositional uniformity is especially critical for flat panel display phosphors in which luminance and threshold voltage are directly related to the composition and local thickness of the active layer.

The phosphor films are deposited onto 2" x 2" glass substrates which are coated with layers of indium tin oxide (electrode) and aluminum titanium oxide (insulator). The effects of chamber pressure, deposition rate, substrate temperature, and processing gas composition on the phosphor film composition, microstructure, and EL performance are currently under investigation. Table I lists the ranges over which these parameters are being studied.

Parameter	Range
Chamber pressure	10 - 30 mTorr
Substrate temperature	250 - 450 °C
H <sub>2</sub> S gas concentration	0 - 2%
Deposition rate	140-700

Table I. Deposition parameters and their ranges for ZnS:Mn and SrS:Ce phosphor films.

The chamber pressure, substrate temperature, and deposition rate have important effects on the resultant thin film composition, crystallinity, and microstructure which all affect EL performance. Several researchers have proposed that the process gas composition also has a significant effect on the film properties. One theory proposes that Ar atoms from the process gas are incorporated into the thin film structure during growth resulting in a reduction in EL performance (27). As a result, some researchers have suggested using a 60% Ar/40% He process gas mixture as a means of reducing either Ar incorporation (28) or surface impact damage to the ZnS

thin film (29). Other researchers have reported that the use of the Ar/He gas mixture does not affect the crystallinity or EL performance of ZnS:Mn phosphor films (14). In this experiment, we compared films deposited using process gases that consisted of Ar only and of a 60% Ar/40% He mixture.

Because ZnS and SrS thin films often are substoichiometric (sulfur deficient), some researchers suggest using a process gas containing 1 - 5% H<sub>2</sub>S to increase the sulfur content which improves stoichiometry, crystallinity, and EL performance in the films (12, 14). We are investigating the effect of adding 0 - 2% H<sub>2</sub>S to the processing gas for both ZnS:Mn and SrS:Ce depositions.

**2.1.1 ZnS:Mn** The ZnS:Mn samples are deposited using a ZnS sputter target containing 0.6 atomic % (0.7 weight %) Mn in the form of MnS. It is important to note that this atomic percentage represents the number of dopant atoms (Mn) compared to the total number of atoms in the target. However, some target manufacturers consider a host material molecule, such as ZnS, to count as a single entity (atom). This results in dopant levels that are a fraction of the specified concentration. To avoid confusion, the dopant concentration should be specified as a weight percentage of the entire target.

**2.1.2 SrS:Ce** The sputter target for the blue phosphor consists of SrS doped with 0.6 atomic % (1.0 weight %) CeF<sub>3</sub>. Because SrS is a hygroscopic material, targets must be handled with extreme care in order to avoid reaction with atmospheric moisture. The use of the load-lock on our sputter chamber minimizes the exposure of this target to atmospheric contamination.

### 3. DISCUSSION

#### 3.1 Performance of Phosphor Films

**3.1.1 ZnS:Mn** The deposition parameters and resultant EL performance values at a 60 Hz driving frequency for several of our sputtered ZnS:Mn thin film phosphors are summarized in Table II.

These data suggest that chamber pressure has a significant effect on luminance output, while deposition rate does not. In addition, we have fabricated samples under identical conditions except for using a 60% Ar/40% He process gas mixture and obtained very similar EL values. This indicates that the use of a Ar/He process gas mixture has little effect on EL performance in general.

Substrate Temp (°C)	Process Gas	Chamber pressure (mTorr)	Dep. rate (Å/min)	Thickness (Å)	Threshold voltage (V)	L <sub>40</sub> (fL)	% Diffuse reflectance
250	Ar	10	480	7500	156	8.5	2.8
250	Ar	10	480	7500	170	9.5	3.1
250	Ar	10	700	7500	164	8.5	2.8
250	Ar	10	700	7500	163	9.2	2.9
250	Ar	30	480	7500	166	16.0	2.9
250	Ar	30	480	7500	168	17.5	3.3
250	Ar	30	700	7500	158	13.0	2.9

Table II. Deposition parameters and EL performance values for sputtered ZnS:Mn phosphor films. L<sub>40</sub> is the luminance output at 40 volts over threshold voltage.

We note that the L<sub>40</sub> values are lower than some of those previously reported (> 27 fL at 60 Hz) for ZnS:Mn samples of comparable thickness under similar test conditions (15). We first suspected that oxygen contamination in these films was reducing luminance output. However, the oxygen content in these films was found to be below limits of detection (< 0.2 atomic %) using electron microprobe (EMP) analysis. Subsequently, we now suspect that our low luminance values may be a result of poor crystallinity or a low Mn dopant concentration (0.6 atomic %). Matsuoka *et al.* reported that the optimum Mn concentration in rf sputtered ZnS:Mn phosphor films is 1.2-1.6 atomic % (13) which is substantially higher than the optimum concentration of 0.6 atomic % reported for thermally evaporated films (30, 31) and used in this research.

Substrate temperature also appears to have an important effect on crystallinity and EL performance. Several preliminary ZnS:Mn films were sputter deposited onto substrates maintained at temperatures ranging from 200 - 500 °C and then analyzed using standard  $\theta$ -2θ X-ray diffraction. The Scherrer equation (32) was used to calculate the average crystallite diameter in each film. Films that were deposited at T < 250 °C exhibited a single diffraction peak which corresponds to the (111) peak of the low temperature cubic (sphalerite) phase of ZnS which is consistent with previous reports (13, 14). Films deposited at much higher temperatures (500 °C) exhibited a similar diffraction peak {hexagonal (0002)} as well as other minor peaks that correspond to the high temperature hexagonal (wurtzite) phase. The average crystallite diameter for the low and high temperature samples was ~ 1000 Å for 5000 Å thick films.

Although the diffraction peaks for the (0002) hexagonal and (111) cubic phase are located at nearly the same 2θ value, we are able to differentiate between the two phases by using a new technique for obtaining powder diffraction data from preferentially oriented thin film samples such as these on a standard  $\theta$ -2θ X-ray diffractometer (33). In addition, we found that ZnS:Mn films deposited at intermediate temperatures (250-300 °C) exhibited powder-type diffraction patterns

from both the hexagonal and cubic phases which is consistent with a report by Xian *et al.*. This mixed phase is likely a result of a thermal transition from the low temperature cubic phase to the high temperature hexagonal phase. The diffraction peaks from the mixed phase samples were much broader indicating a reduction in average crystallite size ( $\sim 200 \text{ \AA}$ ). The combination of diffraction peaks, small crystallite size, and lack of preferred orientation suggests that competition between the two phases during deposition severely limited crystalline growth. The resultant high density of grain boundaries increases the probability for non-radiative recombination of electron-hole pairs, and can reduce the luminescent output significantly. Therefore, ZnS:Mn phosphor films should be deposited on the high temperature side (hexagonal crystal structure) of this thermal phase transition to ensure maximum EL performance.

The ZnS:Mn films exhibit low diffuse reflectance values which indicate that a significant portion of the light produced in the phosphor is waveguided out through the edge of the sample. While this effect contributes to the low luminance output from these samples, it is likely that poor crystallinity and low Mn concentrations are the limiting factors for the overall EL performance. As a result, our future experiments will include the use of a ZnS:Mn target with a higher Mn concentration and depositions at higher substrate temperatures ( $350 \text{ }^{\circ}\text{C}$ ) to enhance crystallinity.

**3.1.2 SrS:Ce** Several preliminary samples of SrS:Ce were deposited onto substrates maintained at temperatures ranging from  $250 - 450 \text{ }^{\circ}\text{C}$  and submitted for EMP analysis. The results indicate that the Ce concentration and S:Sr ratio are unaffected by deposition temperature over the range studied. All films were found to be sulfur deficient (S:Sr ratio =  $.95 \pm .004$ ) but contain significant quantities of oxygen contamination, even in samples capped with a protective layer. Optimum EL performance requires a stoichiometric film with a minimum number of impurities. Therefore, we introduced a 2% concentration of  $\text{H}_2\text{S}$  into the Ar processing gas in order to increase the relative sulfur content in these films. EMP analysis showed an increase in the sulfur and a dramatic decrease (94% reduction) in the oxygen content. Although they were the thinnest samples, these films exhibited the highest luminance of all our SrS:Ce samples. The addition of  $\text{H}_2\text{S}$  gas also had the effect of shifting the CIE color coordinates to a more desirable color of blue for TFEL displays.

The deposition parameters and resultant EL performance values at a 60 Hz driving frequency for some of our sputtered SrS:Ce thin film phosphors deposited with and without  $\text{H}_2\text{S}$  gas are summarized in Table III.

We monitored the partial pressure of  $\text{H}_2\text{S}$ ,  $\text{H}_2\text{O}$ , and  $\text{O}_2$  before, during, and after deposition of the SrS:Ce films using a residual gas analyzer. We observed a significant decrease in  $\text{H}_2\text{S}$  and a corresponding increase in  $\text{H}_2\text{O}$  partial pressures when the plasma was ignited. When the plasma was turned off, the partial pressures returned to their original values. This suggests that the plasma acts as a

Substrate Temp (°C)	Process Gas	H <sub>2</sub> S conc. (%)	Chamber pressure (mTorr)	Dep. rate (Å/min)	Thickness (Å)	Threshold voltage (V)	L <sub>40</sub> (fL)	CIE-x	CIE-y
250	Ar	0	30	400	8900	148	3.6	0.197	0.384
250	Ar	0	30	400	8900	150	2.0	0.184	0.358
250	Ar	0	30	400	9500	158	1.5	0.197	0.369
250	Ar	0	30	400	9500	158	2.1	0.201	0.379
250	Ar	2	30	140	3300	87	5.1	0.271	0.494
250	Ar	2	30	140	3300	96	5.7	0.268	0.489

Table III. Deposition parameters and EL performance values for sputtered SrS:Ce phosphor films.

catalyst to react H<sub>2</sub>S with free oxygen to produce H<sub>2</sub>O and S. The increase in sulfur content of the resultant film supports this theory. Although the addition of H<sub>2</sub>S to the processing gas improves the composition and consequently the EL performance of the SrS:Ce films, it does not fully compensate for the high concentration of oxygen in the sputter chamber and the thin films. Our future research will include experiments to determine and eliminate potential sources of oxygen contamination in our SrS:Ce films.

#### 4. CONCLUSION

We have used rf sputtering to successfully deposit ZnS:Mn and SrS:Ce phosphor films with luminance values of up to 17.5 and 5.7 fL respectively at 60 Hz for use in TFEL devices. We believe that we can achieve higher luminance values for the ZnS:Mn thin films by using higher deposition temperatures (350 °C) to improve crystallinity and higher Mn concentrations. We also plan to investigate and eliminate potential sources of oxygen in our SrS:Ce phosphor films in order to increase their emission. Our ultimate goal is to find a common set of sputter deposition parameters to produce high EL efficiency, multilayered stacks of ZnS:Mn and SrS:Ce phosphor films for use in TFEL flat panel displays. We believe that sputtering is the best deposition method for these displays because it permits a common deposition temperature for ZnS:Mn and SrS:Ce at 300 -350 °C instead of a temperature variation of 300 °C required for other deposition processes. In addition, sputter deposition offers larger panel sizes, higher film densities, higher quality uniformity, higher deposition rates, lower cost, and in-line manufacturing capabilities.

## 5. ACKNOWLEDGMENTS

This work was performed at Sandia National Laboratories and Planar America, Inc. under APR contract DAAL01-94-C-3418.

## 6. REFERENCES

1. New Venture Forecasting (1994).
2. R. Mach and G. O. Mueller, SPIE Proc. 1910, 48 (1993).
3. K. Okabayashi, T. Ogura, K. Terada, K. Taniguchi, T. Yamashita, M. Yoshida, and S. Nakajima, SID Digest, 275, (1991).
4. R. H. Mauch, K. O. Velthaus, H. W. Schock, S. Tanaka, and H. Kobayashi, SID Digest, 178 (1992).
5. R. H. Mauch, K. O. Velthaus, B. Huttel, and H. W. Schock, SID Digest, 769 (1993).
6. T. Mishima, W. Quan-Kun, and K. Takahashi, J. Appl. Phys., 52, 5797 (1981).
7. T. Suntola, J. Anston, A. Pakkala, and S. Lindfors, SID Digest, 108 (1980).
8. A. F. Cattell, B. Cockayne, K. F. Dexter, J. Kirton, and P. J. Wright, Intl. Display Research Conf., 20 (1982).
9. V. S. Ban and E. A. D. White, J. Cryst. Growth, 33, 365 (1976).
10. H. Ohnishi, N. Sakuma, K. Ieyasu, and Y. Hamakawa, J. Electrochem. Soc., 130, 2115 (1983).
11. A. J. Warren, C. B. Thomas, H. S. Reehal, and P. R. C. Stevens, J. Lumin., 28, 147 (1983).
12. M. I. Abdalla, J. L. Plumb, L. L. Hope, SID Digest, 245 (1984).
13. T. Matsuoka, J. Kuwata, M. Nishikawa, Y. Fujita, T. Tohda, and A. Abe, Jap. J. of Appl. Phys., 27, 592 (1988).
14. H. Xian, P. Benalloul, C. Barthou, and J. Benoit, Thin Solid Films, 248, 193 (1994).
15. G. Frey, D. Serafin, and r. Boudreau, SID Digest, 16 (1988).
16. R. H. Mauch, K. O. Velthaus, G. Bilger, H. W. Schock, Proc. of II-VI Conf., (1991).
17. S. Tanaka, H. Morita, K. Yamada, and H. Kobayashi, Intl. Display Research Conf., 137 (1991).
18. H. Ohnishi, R. Iwase, and Y. Yamasaki, SID Digest, 289 (1988).
19. G. O. Mueller, R. Mach, B. Selle, and H. Ohnishi, J. Cryst. Growth, 101, 999 (1990).
20. H. Ohnishi and T. Okuda, SID Digest, 31 (1990).
21. R. Mach, G. O. Mueller, and R. U. Reinsperger, SID Digest, 367 (1992).
22. G. O. Mueller, R. Mach, and H. Ohnishi, Intl. Display Research Conf., 88 (1990).
23. W.A. Barrow, R. E. Coovert, and C. N. King, SID Digest, 249 (1984).
24. T. Nire, A. Matsuno, F. Wada, K. Fuchiwaki, and A. Miyakochi, SID Digest, 352 (1992).

25. K. O. Velthaus, R. H. Mauch, H. W. Schock, S. Tanaka, K. Yamada, K. Ohmi, and H. Kobayashi, Proc. 6th Intl. Workshop on Electroluminescence, 187 (1992).
26. K. Ohmi, S. Tanaka, Y. Yamano, K. Fujimoto, H. Kobayashi, R. H. Mauch, K. O. Velthaus, and H. W. Schock, Tech. Digest of the Japan Displays, 725 (1992).
27. J. L. Vossen and J. J. Cuorno in J. L. Vossen and W. Kern, eds. , Thin Film Processes, Academic Press, New York, 58 (1978).
28. H. Ohnishi, Y. Yamamoto, and Y. Katayama, Proc Intl. Display Research Conf., 159 (1985).
29. K. Okamoto, T. Yoshimi, K. Nakamura, T. Kobayashi, S. Sato, and S. Miura, Jap. J. Appl. Phys., 28, 1378 (1989).
30. V. Marrelo and A. Onton, IEEE Trans. Electron. Devices ED, 27, 1767 (1980).
31. H. Sasakura, H. Kobayashi, S. Tanaka, J. Mita, T. Tanaka, and H. Nakayama, J. Appl. Phys., 52, 6901 (1981).
32. B. D. Cullity, Elements of X-Ray Diffraction, Addison-Wesley, Menlo Park (1978).
33. M. Rodriguez and J. A. Ruffner, J. Vac. Sci. Tech., to be published.